Available online at www.sciencedirect.com
ScienceDirect
Chinese Journal of Natural Medicines 2019, **17**(12): 0970–0981
Chinese Journal of Natural Medicines

Structural determination of eleven new preschisanartane-type schinortriterpenoids from two *Schisandra* species and structural revision of preschisanartanin J using NMR computation method

HU Kun, LI Xing-Ren, TANG Jian-Wei, Li Xiao-Nian, PUNO Pema-Tenzin*

State Key Laboratory of Phytochemistry and Plant Resources in West China, Kunming Institute of Botany, Chinese Academy of Sciences, Kunming 650201, China

Available online 20 Dec., 2019

[ABSTRACT] Nineteen preschisanartane-type schinortriterpenoids (SNTs), among which eleven ones were previously undescribed, were isolated from two *Schisandra* species, *S. sphaerandra* and *S. rubriflora*. Their structures were determined using 1D and 2D NMR spectroscopic analyses, NMR data comparison, quantum chemical calculation of NMR parameters, electronic circular dichroism (ECD), X-ray single crystal diffraction, and chemical derivation. Furthermore, structural re-examination of a few previously reported preschisanartane-type SNTs led to the structural revision of preschisanartanin J. Besides, it is suggested that the reported structures of arisanlactone D and schilancidilactone W should be re-checked. Finally, a few isolated SNTs were found to possess neurite outgrowth-promoting activities, and protective activities against neural injuries.

[KEY WORDS] *Schisandra sphaerandra*; *Schisandra rubriflora*; Preschisanartane-type schinortriterpenoids; Structural revision; Quantum chemical calculation of NMR parameters

[CLC Number] R284 **[Document code]** A **[Article ID]** 2095-6975(2019)12-0970-12

Introduction

Schinortriterpenoids (SNTs) is a class of structurally diverse triterpenoids exclusively found in the Schisandraceae plants, more specifically in the genus *Schisandra* [1-2]. The report of micrandilactone A [3-4] in 2003 from our group marked the debut of SNTs. Up to now, more than 200 SNTs categorized into over 20 biosynthetically related types have been reported [1-2]. These structurally intricate molecules have aroused great interests among synthetic organic chemists, and many cases of total synthesis have been published [5-6]. Meanwhile, the complicated scaffolds, abundant chiral centers, and flexible side chains in SNTs also posed great challenges to their structural determination, which can be reflected by the previous structural misassignments of rubriflordilactone B [7-8], propindilactone G [9-10] and arisanlactone A [11-12].

Our recent phytochemical investigations on two *Schisandra* species, *S. sphaerandra* Stapf and *S. rubriflora* (Franch). Rehd. et Wils, has resulted in the isolation of nineteen preschisanartane-type SNTs, among which 11 ones were previously unreported (Fig. 1). Preschisanartane-type SNTs, characterized by a 7/8/3 ring system, constituted a medium group of SNTs with only twenty-one members reported previously (Fig. S1) [1-2, 13]. In the present research, compounds **1** and **2** were found to possess rare 17*S* configurations. Moreover, unusual hydroxyl substitutions at C-1, C-8 were found in **3**–**6**. The structures of new compounds were determined mainly using 1D and 2D NMR spectroscopic analysis, NMR data comparison, quantum chemical calculation of NMR parameters, electronic circular dichroism (ECD), X-ray single crystal diffraction, and chemical derivation. While the structures of those known compounds, including preschisanartanin J (**12**) [14], preschisanartanin B (**15**) [15], schilancidilactone W (**16**) [16], preschisanartanin A (**18**) [17], preschisanartanin D (**19**) [18], preschisanartanin O (**20**) [19], 2*β*-hydroxyarisanlactone C (**21**) [12], schilancidilactone V (**22**) [16], were elucidated mainly by NMR data comparison with those reported in literatures. Furthermore, a re-examination of selected molecules in previously

[Received on] 03-Sep.-2019
[Research funding] This work was supported by the National Natural Science Foundation of China (No. 81903520) and the Second Tibetan Plateau Scientific Expedition and Research (STEP) program (No. 2019QZKK0502).
[*Corresponding author] E-mail: punopematenzin@mail.kib.ac.cn
These authors have no conflict of interest to declare.
Dedicated to Professor SUN Han-Dong on the Occasion of His 80th Birthday

reported preschisanartanes using NMR computation method has led to the structural revision of preschisanartanin J. Moreover, it is suggested that the reported structures of arisanlactone D [12] and schilancidilactone W [16] should be re-checked.

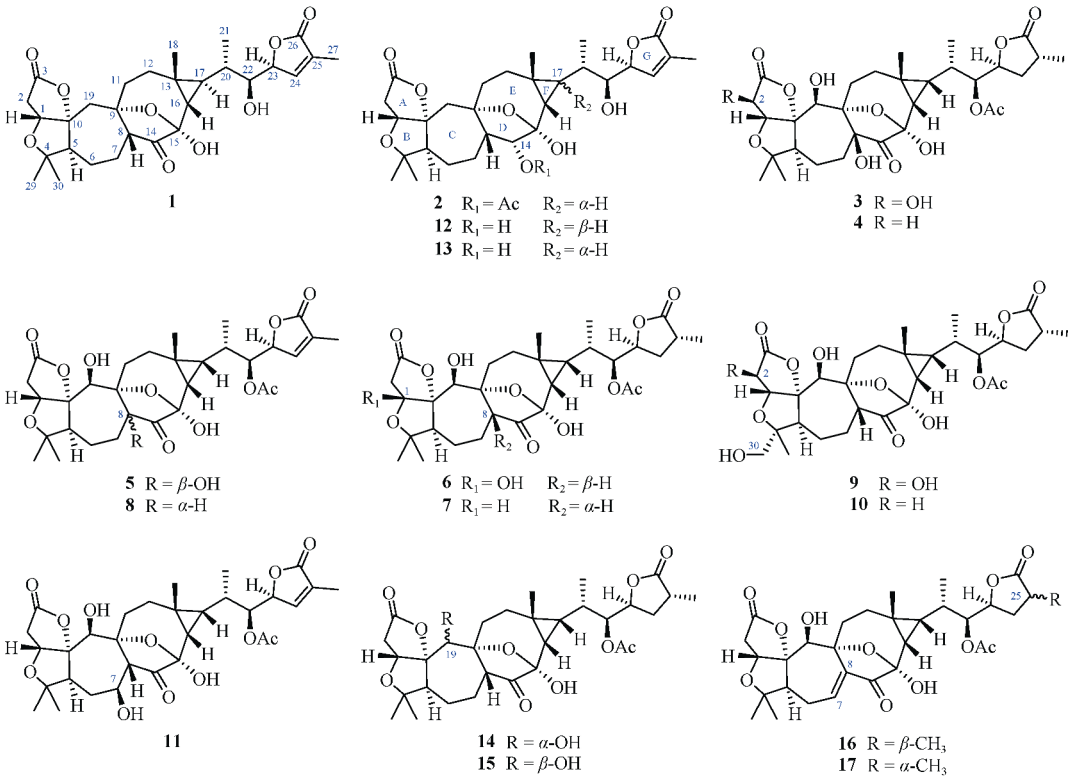

Fig. 1 Structures of 11 new preschisanartane-type SNTs from *S. sphaerandra* and *S. rubriflora* (1–11); Originally proposed and revised structures of preschisanartanin J (12, 13, respectively); Originally proposed structures of arisanlactone D (14) and schilancidilactone W (16), and their suggested right structures (15 and 17, respectively)

Results and Discussion

Preschisanartanin Q (**1**) was isolated as a white powder. Its molecular formula was determined as $C_{29}H_{38}O_9$ by HRESI-MS (*m/z* 553.2408 $[M + Na]^+$, Calcd. 553.2408), indicating 11 degrees of unsaturation. The ^{1}H NMR spectrum of **1** displayed 1 secondary methyl at δ_H 1.13, and 4 tertiary ones at δ_H 0.93, 1.01, 1.14 and 1.82. The ^{13}C NMR and DEPT spectra showed 29 carbon resonances, including 5 methyls, 6 methylenes, 9 methines (1 olefinic and 3 oxygenated carbons), and 9 nonprotonated carbons (1 carbonyl group, 2 ester groups, 1 olefinic carbons, 4 oxygenated carbons, and 1 quaternary carbon). The above evidences, in addition to the characteristic signals of the cyclopropane ring (δ_C 24.0, C, C-13; 36.0, CH, C-16; 29.7, CH, C-17; δ_H 1.34, d, H-16; 1.58, dd, H-17), indicated that **1** was an SNT with prescisanartane scaffold. Analysis of the HSQC spectrum of **1** enabled all proton signals to be unambiguously assigned to their respective carbons. Subsequent comprehensive analysis of the HMBC and ^{1}H-^{1}H COSY spectra revealed that **1** shared similar planar structure with that of the previously reported preschisanartanin O (**20**) [19], except that **1** has one less oxygenated methine and one more methylene than the latter. In consideration of their same degree of unsaturation and the 16 Dalton difference in molecular weight, **1** was initially thought as the 19-dehydroxy preschisanartanin O, as suggested by HMBC correlations from H_2-19 (δ_H 2.09, 2.45) to C-9 (δ_C 78.2), C-10 (δ_C 96.2), C-5 (δ_C 62.2), C-8 (δ_C 56.1), C-1 (δ_C 81.6).

The stereochemistry of the left part of **1** was determined by NMR data comparison with those of preschisanartanin O, as well as the H_3-29/H-1β, H-5/H_3-30α, and H-8/H-6β/H_3-29β ROESY correlation. As for the right part, H-16/H_3-18β ROESY correlation revealed H-16 to be β-oriented. However, it was surprising that neither H-16 nor H_3-18 displayed ROESY correlations with H-17, furthermore, the $^3J_{H\text{-}16/H\text{-}17}$ (5.5 Hz) in **1** didn't fall within the range of 7.0−9.7 Hz as in reported preschisanartanes. The above evidences implied that H-16 and H-17 in **1** were unexpectedly in *trans* arrangement on the strained cyclopropane ring, as in three fungus-derived sesquiterpenoids, hypocoprins A−C [20]. Moreover, the diagnostic Cotton effect around 210 nm in the ECD spectra of **1** enabled C-23 to be assigned as *S* configuration via empirical rule [21]. Thus, the remaining questions for structural determination of **1** involved the validation of its unusual C-17 stereochemistry, as well as the configuration determination of C-20 and C-22 in the flexible side chain, which is usually conserved (20*S*, 22*S*). Then, all the 4 possible candidates of **1** (represented by configurations of C-20 and C-22, with other

chiral centers being equal, that is, 1R^*, 5S^*, 8R^*, 9S^*, 10R^*, 13R^*, 15S^*, 16S^*, 17S^*, 23S^*), (20S^*, 22S^*)-**1** (**1a**), (20R^*, 22S^*)-**1** (**1b**), (20S^*, 22R^*)-**1** (**1c**), (20R^*, 22R^*)-**1** (**1d**), were subjected to quantum chemical calculation of NMR chemical shifts, under the theory level of MPW1PW91-SCRF/6-31G(d, p)//B3LYP/6-31G(d) with IEFPCM solvent model. As a result, the calculated data of **1a** agreed with the experimental data best. Furthermore, among the 4 sets of calculated data, the DP4+ probability (all data) [22] of **1a** being 100% definitely exclude all the three other possibilities (Table 1). The coupling constant of $^3J_{\text{H-16/H-17}}$ in **1a** were also calculated, and the result (5.8 Hz) were in good agreement with the experimental one (5.5 Hz), while the calculated $^3J_{\text{H-16/H-17}}$ for preschisanartanin O (**20**) using the same method was 8.9 Hz (the experimental counterpart was 8.7 Hz). In combination with biosynthetic considerations, the absolute configuration of **1** was finally determined as 1*R*, 5*S*, 8*R*, 9*S*, 10*R*, 13*R*, 15*S*, 16*S*, 17*S*, 20*S*, 22*S*, and 23*S*.

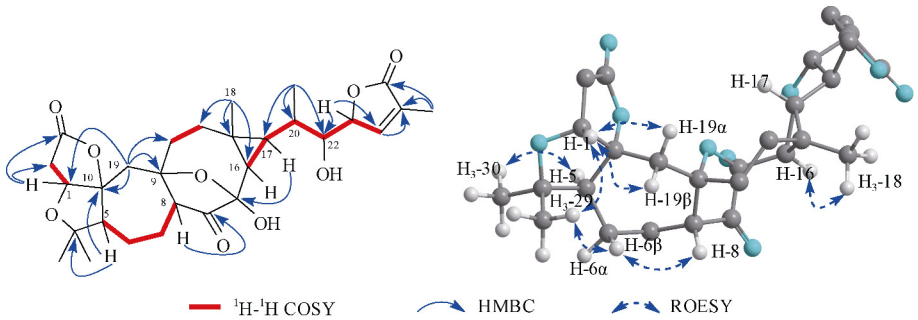

Fig. 2 Key ^{1}H-^{1}H COSY, HMBC, and ROESY correlations of 1 (only relevant hydrogens were presented in the 3D molecular model for clarity, similarly hereinafter)

Table 1 Analysis of the NMR computation results of 1a–1d

Stereoisomers	^{13}C NMR			^{1}H NMR			DP4+ (all data)
	R^2	MAE	CMAE	R^2	MAE	CMAE	
1a	0.9994	1.3	1.0	0.9795	0.18	0.17	100%
1b	0.9987	1.5	1.5	0.9768	0.17	0.17	0%
1c	0.9987	1.7	1.4	0.9681	0.19	0.20	0%
1d	0.9987	1.6	1.6	0.9706	0.19	0.19	0%

Preschisanartanin R (**2**) was isolated as a white powder. The molecular formula $C_{31}H_{42}O_{10}$ was determined by HRESI-MS (*m/z* 613.2413 [M + K]$^+$, Calcd. 613.2410). The NMR spectra of **2** were highly similar to those of **1**, except that the typical carbonyl signal attributed to C-14 was not observed in the ^{13}C spectrum of **2** and was replaced by an acetoxyl group substituted methine, which was supported by HMBC correlations from H-14 (δ_H 5.58) to C-7 (δ_C 23.7), C-8 (δ_C 50.9), C-15 (δ_C 101.7), C-16 (δ_C 39.7), and the acetoxyl group (δ_C 170.3). The configuration of **2** was mainly established by NMR data comparison with those of **1** and by ROESY correlations. As for the newly emerged chiral center of C-14 in **2**, the ROESY correlations of H-14 with H-16*β* (δ_H 1.41), H-8*β* (δ_H 2.36) indicated they are all co-facial. Finally, the $^3J_{\text{H-16/H-17}}$ (5.8 Hz) manifested that **2** also had 17*S* configuration as **1**. A subsequent NMR computation of the established structure of **2** strongly supported its correctness (Table S1).

Preschisanartanin S (**3**) was isolated as a white powder. The molecular formula $C_{31}H_{42}O_{13}$ was determined by HRESI-MS (*m/z* 645.2511 [M + Na]$^+$, Calcd. 645.2518). Diagnostic signals of the cyclopropane ring (δ_C 26.0, C, C-13; 30.8, CH, C-16; 33.2, CH, C-17; δ_H 1.55, d, H-16; 1.06, m, H-17) were also observed in NMR spectra of **3**, indicating it to be a prescisanartane-type SNT. The NMR data of **3** implied its structure to be highly similar to that of 2*β*-hydroxyarisanlactone C [12], with the only difference being that the C-8 methine in the latter changed into a hydroxylated nonprotonated carbon in **3**, which can be confirmed by HMBC correlations from HO-8 (δ_H 7.55, s) to C-8 (δ_C 82.4, C) and C-14 (δ_C 216.9, C) (Fig. 3). As for the stereochemistry of **3**, despite the lack of ROESY evidences, the H-2 can be assigned as *α*-oriented according to the singlet peak of H-1 (δ_H 5.17) in the ^{1}H spectrum, indicating the H-1/C-1/C-2/H-2 dihedral to be around 90°. The ROESY correlations of H-16/H$_3$-18*β*, H-17/H-16, as well as the $^3J_{\text{H-16/H17}}$ (9.0 Hz) implied they are all co-facial. However, the configurational determination of C-8, C-19, and chiral centers on the flexible side chain was hampered by lack of solid evidences. Fortunately, a single crystal of **3** was obtained, which established the whole structure of **3** (CCDC number: 1942580) (Fig. 3).

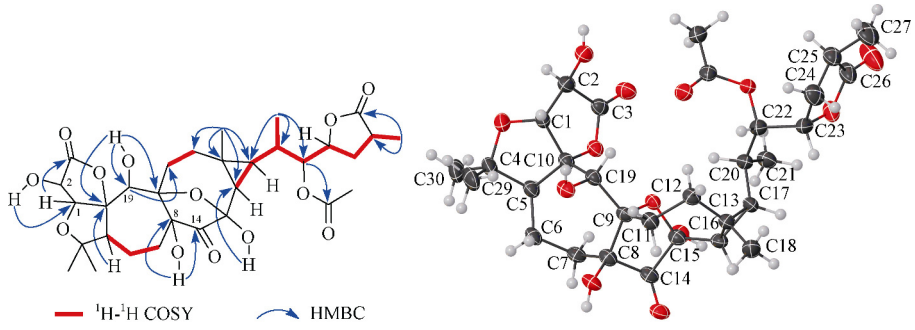

Fig. 3 Left: key ^{1}H-^{1}H COSY and HMBC correlations of 3; Right: the X-ray crystallographic structure of 3

Preschisanartanin T (**4**) was isolated as a white powder. The molecular formula $C_{31}H_{42}O_{12}$ was determined by HRESI-MS (*m/z* 605.2610 $[M + Na]^+$, Calcd. 605.2604). In consideration of the 16 Dalton difference between molecular weights of **4** and **3**, and their similarity in NMR data, **4** was deduced as the C-2 dehydroxylated form of **3**, which can be proved by HMBC correlation between H_2-2 (δ_H 2.78, 3.40) and C-3 (δ_C 175.6, C). The configuration of the left part of **4** can be determined by ROESY correlations and NMR data comparison with those of **3**. Meanwhile, the configurations of C-20, C-22, and C-23 are usually conserved in preschisanartanes. However, no useful ROESY correlations existed for the configurational determination of C-25. Moreover, strictly speaking, configurational determination of C-25 in **4** through mere NMR data comparison with those of **3** was not practically feasible, because NMR data discrepancy between two possible C-25 epimers was not known. This may be also the reason that the stereochemistry of C-25 in preschisanartanins B and D were left undetermined (Fig. S1). To settle this issue, preschisanartanins A (**18**) and O (**20**) were reduced with H_2 under Pd/C catalyst, respectively. Surprisingly, only one main product was obtained for each reaction (Scheme 1). They had similar NMR spectra with preschisanartanin B (**15**) [15] and arisanlactone C [12], respectively, however, still subtle differences can be observed in NMR data ascribed to furan-rings on the side chains (Table S7). They were finally assigned as 25-*epi*-prescisanartanin B and 25-*epi*-arisanlactone C, respectively, based on comprehensive 1D and 2D NMR data analysis, especially the H-23/H-25 ROESY correlations observed in the spectra of both compounds. Thus, NMR data comparison was safely undertaken to find that NMR data of the side chains in **4** and preschisanartanin D (**19**) [18] were well consistent with those of preschisanartanin B. In combination with the absence of H-23/H-25 ROESY correlations in **4** and **19**, C-25 in these compounds were all assigned as 25*R*.

Preschisanartanin U (**5**) was isolated as a white powder. The molecular formula of $C_{31}H_{40}O_{12}$, with 12 indices of hydrogen deficiency, was determined by HRESI-MS (*m/z* 717.2384 $[M + CF_3COO]^-$, Calcd. 717.2376). The NMR data of **5** were extremely similar to that of the **4**, except that the C-24/C-25 bond in the latter was replaced by a pair of double bond (δ_C 147.1, C-24; 130.7, C-25; δ_H 7.11, H-24), as proved by HMBC correlations from H-24 to C-23 (δ_C 80.6, CH), C-25 and C-27 (δ_C 10.5). The strong Cotton effect around 210 nm in the ECD spectrum of **5** manifested the absolute configuration of C-23 to be *S*.

Preschisanartanin V (**6**) was isolated as a white powder. The molecular formula of $C_{31}H_{42}O_{12}$, with 11 indices of hydrogen deficiency, was determined by HRESI-MS (*m/z* 605.2617 $[M - H]^-$, Calcd. 605.2604). The NMR data of **6** were extremely similar to those of the previously reported preschisanartanin B (**15**), except that an oxygenated methine in the latter was taken place by an ketal carbon (δ_C 110.6, C) in **6**, which was assigned as C-1 according to HMBC correlation of HO-1 (δ_H 7.36) with C-1, C-10 (δ_C 96.2), and of H_2-2 (δ_H 2.70, 3.13) with C-1 and C-3 (δ_C 171.9, C). Moreover, in the ROESY spectrum of **6**, the observed correlation between HO-1 and HO-19*β* indicated C-1 to be in *R* configuration. Furthermore, as in compound **4**, the configuration of C-25 was assigned as *R* by NMR data comparison with those of preschisanartanin B. The established structure of **6** was also subjected to NMR computation, and the calculated chemical shifts matched their experimental counterparts very well (Table S1).

Preschisanartanin W (**7**) was isolated as a white powder. The molecular formula $C_{31}H_{42}O_{11}$ was determined by HRESI-MS (*m/z* 625.2433 $[M + Cl]^-$, Calcd. 625.2411). Thorough analysis of the 1D, HMBC, and ^{1}H-^{1}H COSY NMR spectra of **7** (Fig. 4) revealed that it shared the same planar structure with preschisanartanin B, however, those data attributed to rings C and D differed obviously. In the ROESY spectrum, the H-29 (δ_H 1.31)/H-1*β* (δ_H 5.10), H-5 (δ_H 2.11)/H_3-30*α* (δ_H 1.22), H-8 (δ_H 3.82)/H-5, and H-19 (δ_H 4.59)/H-8 correlations indicated that H-8 and H-19 were both *α*-oriented as H-5 (Fig. 4). Finally, the configuration of C-25 was determined as the same with prescisanartanin B. The established structure of **7**, especially the unusual C-8 stereochemistry, was supported by quantum chemical calculation of NMR chemical shifts (Table S1**)**.

Preschisanartanin X (**8**) was isolated as a white powder. The molecular formula $C_{31}H_{40}O_{11}$ was determined by HRESIMS (*m/z* 623.2259 $[M + Cl]^-$, Calcd. 623.2265). According to elaborate spectrum analyses, **8** was found to possess nearly the same structure and stereochemistry with **7**,

except that the C-24/C-25 bond in **8** was replaced by a pair of double bond (δ_C 146.9, C-24; δ_C 130.5, C-25; δ_H 7.09, H-24), which can be demonstrated by HMBC correlations from H-24 to C-23 (δ_C 80.4), C-25 and C-27 (δ_C 10.5). The strong Cotton effect around 210 nm in the ECD spectrum of **8** manifested the configuration of C-23 to be *S*.

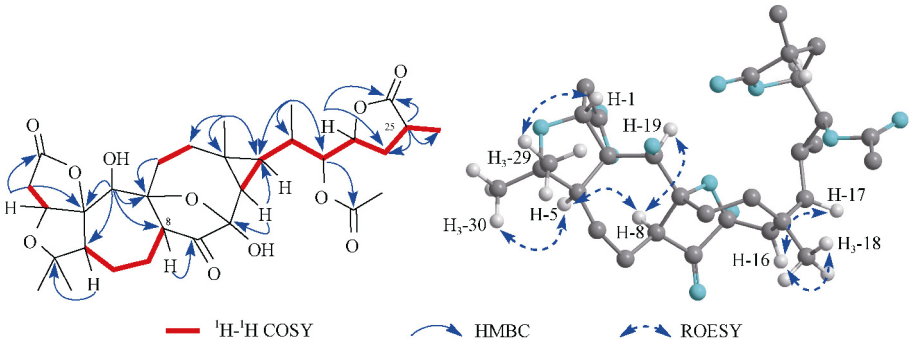

Fig. 4 Key ^{1}H-^{1}H COSY, HMBC, and ROESY correlations of 7

Preschisanartanin Y (**9**) was isolated as a white powder. The molecular formula $C_{31}H_{42}O_{13}$ was determined by HRESI-MS (*m/z* 645.2517 $[M + Na]^+$, Calcd. 645.2518). The ^{1}H NMR spectrum of **9** displayed 2 secondary methyls at δ_H 1.14, 1.80 ppm, and 3 tertiary ones at δ_H 1.02, 1.48, and 2.10 ppm. The ^{13}C NMR and DEPT spectra showed 31 carbon resonances, including 5 methyls, 6 methylenes (1 oxygenated one), 11 methines (5 oxygenated carbons), and 9 nonprotonated carbons (1 carbonyl group, 3 ester groups, 4 oxygenated carbons, and 1 quaternary carbon). The right part of the structure of **9** was assigned as the same as that of prescisanartanin B through careful NMR data analysis. Moreover, the special oxygenated methine was attributed to C-30 based on HMBC correlations from H_2-30 (δ_H 3.63, 3.81) to C-29 (δ_C 17.8), C-4 (δ_C 88.4), and C-5 (δ_C 55.6). The HMBC correlations between H-2 (δ_H 4.61) and C-1 (δ_C 85.5), from H-19 (δ_H 4.64) to C-5, C-9 (δ_C 82.8), C-10 (δ_C 98.5), and C-11 (δ_C 38.3), displayed that C-2 and C-19 were both hydroxylated (Fig. 5). The H-2 was assigned as *α*-oriented owing to the singlet pattern of H-1 (δ_H 5.19) in the ^{1}H spectrum. The H_3-29 (δ_H 1.48)/H-1*β* (δ_H 5.19), H-5 (δ_H 2.99)/H_2-30 clarified the configuration of C-4, C-5. Finally, the structure of **9** were confirmed by single crystal diffraction, and its absolute configuration was determined as 1*R*, 2*R*, 4*R*, 5*S*, 8*R*, 9*R*, 10*S*, 13*R*, 15*S*, 16*S*, 17*R*, 19*S*, 20*S*, 22*S*, 23*S*, and 25*R* (CCDC number: 1942582, Fig. 5).

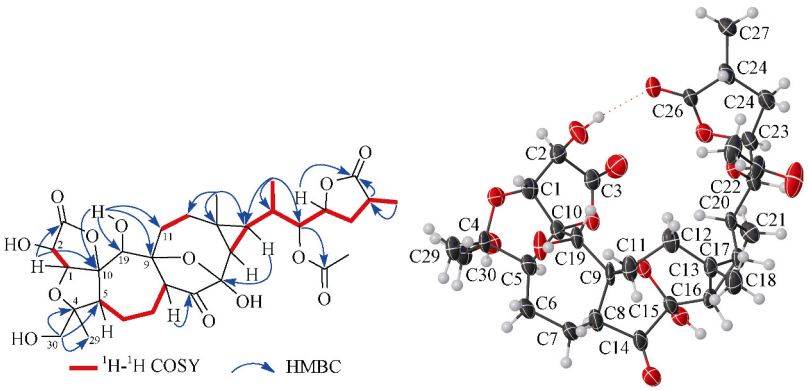

Fig. 5 Left: key ^{1}H-^{1}H COSY and HMBC correlations of 9; Right: the X-ray crystallographic structure of 9

Preschisanartanin Z (**10**) has the chemical formula $C_{31}H_{42}O_{12}$, as indicated by HRESI-MS ion peak at 629.2564 $[M + Na]^+$ (Calcd. 629.2568). **10** was structurally similar to **9** based on their NMR data comparison, except that it possessed one more methylene and one less oxygenated methine than the latter. **10** was then assigned as the 2-dehydroxy analogue of **9**, as deduced by HMBC correlations from H_2-2 (δ_H 2.67, 3.36) to C-1 (δ_C 79.7), C-3 (δ_C 175.5), and C-10 (δ_C 98.6). All chiral centers of **9** were determined to have the same configuration with **9** through NMR data comparison as well as ROESY spectrum analysis.

Preschidilactone A (**11**) possessed a molecular formula of $C_{31}H_{40}O_{12}$, which was determined by the (+)-HRESI-MS ion peak at *m/z* 627.2421 $[M + Na]^+$ (Calcd. 627.2412). **11** possessed similar NMR data with those of preschisanartanin D, except that one methylene and one methine assigned to C-24 and C-25, respectively, in the latter changed into a pair of double bonds (δ_C 130.6, 147.0) in **11**. The diagnostic Cotton effect around 210 nm in the ECD spectrum of **11** manifested the configuration of C-23 to be *S*.

In consideration of the robustness of NMR calculation in the structural determination of this class of molecules, the structures of a number of reported preschisanartanes (those featuring *α*, *β*, *γ*, *δ*-unsaturated-*γ*-lactone in the side chain were excluded here) were re-examined (Fig. S1). Two compounds, preschisanartanin J and arisanlactone D, were found to produce correlative parameters (R^2, MAE, CMAE) that deviated far from the standard established using **18**, **20**, and arisanlactone C, whose structures had been validated by single crystal crystallography (Table S1). Then, the relative data of preschisanartanin J (**12**) and arisanlactone D, especially their NMR data, were re-analyzed.

For preschisanartanin J (**12**), a replicate sample was obtained in the present research. 1D and 2D NMR analysis succeeded in validating the previously established planar structure of originally proposed structure as well as the stereochemistry of rings A−E (Fig. 1), except that the ^{1}H chemical shift of H-16 and H-17 in the original paper were misassigned and should be exchanged (Tables S2 and S3). Furthermore, the NMR data assigned to the right part were highly similar to those of **2**, together with the observed $^3J_{\text{H-16/H-17}}$ of 5.8 Hz (not reported in the original paper due to ^{1}H signal overlap), we assumed that the correct structure of preschisanartanin J should possess a 17*S* configuration (**13**) instead of the previously assigned 17*R* (**12**). The assumption was then confirmed by NMR computation of (1*R*, 5*S*, 8*S*, 9*S*, 10*R*, 13*R*, 14*R*, 15*S*, 16*S*, 17*S*, 20*S*, 22*S*, 23*S*)-preschisanartanin J, which returned well consistent calculated data with the experimental data (Tables S1–S3).

Table 2 ^{13}C NMR (125 MHz) data for compounds 1–11

Position	1 [a]	2 [a]	3 [a]	4 [a]	5 [a]	6 [b]	7 [a]	8 [a]	9 [a]	10 [a]	11 [a]
1	81.6	81.6	84.8	79.3	79.3	110.6	78.1	78.2	85.5	79.7	79.4
2	35.6	35.7	72.9	35.4	35.5	42.5	35.7	35.7	72.9	35.3	35.3
3	175.7	175.8	176.4	175.6 C	175.6	171.9	175.0	175.0	176.4	175.5	175.4
4	83.4	83.6	85.0	84.1 C	84.1	85.9	83.8	83.8	88.4	87.5	84.4
5	62.2	61.9	61.8	62.3	62.3	62.8	60.0	60.1	55.6	56.2	57.9
6	24.2	24.2	20.0	19.9	19.9	24.1	21.8	21.8	24.0	24.0	35.9
7	26.4	23.7	33.8	33.6	33.6	27.4	21.8	21.8	27.3	27.1	68.9
8	56.1	50.9	82.4	82.4 C	83.6	56.2	52.0	52.1	56.4	56.6	63.9
9	78.2	79.8	83.4	83.5 C	82.4	82.4	82.8	82.9	82.8	82.6	81.2
10	96.2	96.7	98.6	98.6 C	98.6	96.2	100.0	100.0	98.5	98.6	97.8
11	42.4	40.3	33.5	33.2	33.4	38.7	29.6	29.7	38.3	38.3	38.0
12	31.1	31.5	24.3	24.0	24.2	25.4	26.0	26.1	25.1	24.8	24.9
13	24.0	24.3	26.0	25.9	26.2	26.3	25.9	26.0	25.9	25.8	25.7
14	216.2	79.7	216.9	217.3	217.3	214.7	215.5	215.6	216.1	216.2	213.4
15	98.8	101.7	98.0	97.9	97.9	99.3	100.5	100.5	99.2	99.1	98.9
16	36.0	39.7	30.8	30.9	31.1	30.9	31.0	31.1	31.2	31.2	31.6
17	29.7	32.7	33.2	33.6	33.6	34.8	35.4	36.0	34.0	34.3	34.3
18	20.8	21.0	28.3	28.4	28.5	28.4	28.2	28.3	28.3	28.3	28.5
19	42.6	42.3	73.3	72.0	72.0	72.5	74.4	74.3	71.9	70.7	70.5
20	37.6	37.6	31.3	31.0	31.3	31.1	31.6	31.8	31.3	31.0	31.1
21	17.6	17.4	18.4	17.8	17.9	17.7	17.9	17.8	18.2	17.7	17.8
22	76.5	76.2	78.8	79.8	76.1	79.9	79.4	76.5	78.8	79.9	76.2
23	82.3	81.7	77.2	76.6	80.6	76.7	76.5	80.4	77.1	76.7	80.6
24	148.6	148.8	33.3	33.4	147.1	33.7	32.8	146.9	33.2	33.2	147.0
25	129.9	129.5	34.1	34.3	130.7	34.6	34.1	130.5	34.1	34.3	130.6
26	174.8	174.9	180.4	180.3	174.3	180.2	179.9	174.1	180.3	180.3	174.3
27	10.7	10.6	16.1	16.5	10.5	16.6	16.3	10.5	16.1	16.5	10.5
29	21.1	21.3	21.9	21.9	21.9	25.4	21.3	21.3	17.8	17.7	21.9
30	27.9	28.2	28.4	28.5	28.5	30.1	27.8	27.8	67.7	67.9	28.4
-OAc		170.3	170.9	170.7 C	170.4	170.8	170.4	170.1	170.8	170.6	170.4
		20.9	21.2	21.5	21.0	21.5	21.1	20.7	21.1	21.5	21.0

[a] Recorded in pyridine-d_5; [b] Recorded in acetone-d_6

Table 3 ^{1}H NMR (600 MHz) data for compounds 1–4 (recorded in pyridine-d_5)

Position	1	2	3	4
1	4.21 (d, 6.0)	4.21 (d, 5.8)	5.17 s	5.14 (d, 5.4)
2a	3.09 (dd, 18.2, 6.0)	3.13 (dd, 18.1, 5.8)	4.70 (d, 4.0)	3.40 (dd, 17.8, 5.5)
2b	2.72 (d, 18.2)	2.74 (d, 18.1)		2.78 overlap
5	2.06 m	2.04 (dd, 13.2, 4.8)	2.35 overlap	2.33 overlap
6a	1.50 overlap	1.47 m	2.94 overlap	2.90 m
6b	1.29 m	1.21 overlap	1.35 m	1.35 m
7a	1.86 m	1.74 m	2.94 overlap	2.90 overlap
7b	1.50 overlap	1.70 m	2.22 overlap	2.90 overlap
8	2.58 (dd, 13.0, 5.4)	2.36 (ddd, 12.4, 7.2, 5.0)		
11a	1.81 m	1.65 m	2.79 m	2.78 overlap
11b	1.67 (dd, 14.3, 8.6)	1.57 m	2.74 m	2.33 overlap
12a	1.92 m	1.72 m	2.28 m	2.54 (t, 13.6)
12b	1.82 m	1.55 m	1.47 (dd, 13.9, 6.6)	1.49 m
14		5.58 (d, 7.2)		
16	1.34 (d, 5.5)	1.41 (d, 5.8)	1.55 (d, 9.0)	1.49 m
17	1.58 (dd, 10.5, 5.5)	1.21 overlap	1.06 m	0.93 (dd, 11.3, 8.9)
18	0.93 s	0.97 s	1.01 s	0.98 s
19a	2.45 (d, 15.8)	2.29 (d, 15.6)	4.76 (d, 7.5)	4.38 (d, 7.6)
19b	2.09 m	1.96 (d, 15.6)		
20	1.74 m	1.66 m	3.36 (dt, 12.0, 6.5)	3.63 m
21	1.13 m	1.02 (d, 6.7)	1.85 (d, 6.5)	1.77 (d, 6.6)
22	3.62 m	3.52 (dd, 8.6, 2.6)	5.26 (t, 5.7)	5.06 (dd, 8.0, 2.3)
23	5.44 s	5.23 q (2.1)	4.92 m	5.02 m
24a	7.22 m	7.14 (t, 1.7)	2.35 overlap	2.19 m
24b			1.99 m	1.95 (dt, 13.1, 8.6)
25			2.78 overlap	2.82 m
27	1.82 s	1.81 (t, 1.7)	1.15 (d, 7.2)	1.20 (d, 7.4)
29	1.01 s	1.03 s	1.38 s	1.38 s
30	1.14 m	1.18 s	1.20 s	1.21 s
-OAc		2.19 s	2.11 s	2.16 s
-OH		6.11 s (HO-22) 8.44 s (HO-15)	7.55 s (HO-8) 7.92 (d, 4.0) (HO-2) 8.19 (d, 7.6) (HO-19) 9.15 s (HO-15)	7.62 s (HO-8) 7.97 (d, 7.6) (HO-19) 9.05 s (HO-15)

Arisanlactone D (**14**) [12] was reported to have an HO-19α, or as the C-19-epimer of preschisanartanin B. However, the difference between the NMR data of arisanlactone D and preschisanartanin B (their NMR data in $CDCl_3$ were extracted from the "experimental section" of the original paper) was nearly negligible [MAD-δ_H = 0.03 ppm; MAD-δ_C = 0.1 ppm; $(\Delta\delta_H)_{max}$ = 0.12 ppm; $(\Delta\delta_C)_{max}$ = 0.4 ppm], even in those atoms around C-19 (Tables S4 and S5). Under this circumstance, the claimed epimerism between the two compounds was obviously unreasonable. Besides, the original sample may suffer from purity problem, which can be reflected by the low signal/noise ratio in the NMR spectra provided in the supporting information. Thus, the ROESY correlations used for configuration determination of C-19, as well as the claimed differences in IR and OR between arisanlactone D and preschisanartanin B in the original paper may be unreliable. In conclusion, arisanlactone D is highly possibly a replicate of preschisanartanin B. However, as we don't have the sample of this compound, we suggest the isolation group to re-check the data and structure of this compound.

Besides, NMR data of schilancidilactone W (**16**) isolated in our research were nearly the same with those reported in

the original paper [16] (Table S6), with their chemical shift discrepancies much lower than those between arisanlactone C and 25-*epi*-arisanlactone C. Furthermore, as no H-23/H-25 ROESY correlation was observed in the present research, we considered that schilancidilactone W may adopted a 25*R* configuration (**17**). However, as no supporting information including the NMR spectra was provided in the original paper, we suggest the isolation group to re-check the data and structure of schilancidilactone W, especially those concerning the configuration of C-25.

Table 4 ^{1}H NMR (600 MHz) data for compounds 5–8

Position	5 [a]	6 [b]	7 [a]	8 [a]
1	5.14 (d, 5.3)		5.10 m	5.12 (dd, 4.2, 2.0)
2a	3.40 (dd, 17.8, 5.5)	2.70 m	2.69 m	2.68 overlap
2b	2.77 m	3.13 (d, 17.2)	2.73 m	2.68 overlap
5	2.34 m	2.42 (dd, 13.1, 5.6)	2.11 (dd, 13.0, 2.0)	2.12 (dd, 13.1, 2.4)
6a	2.91 m	2.26 m	1.69 m	1.66 m
6b	1.35 m	1.55 m	1.32 m	1.34 m
7a	2.90 m	1.99 m	1.84 overlap	1.84 overlap
7b	2.20 m	1.82 m	1.84 overlap	1.84 overlap
8		2.28 m	3.82 (t, 8.7)	3.84 (d, 8.8)
11a	2.78 m	2.53 (dd, 15.2, 6.5)	3.06 m	3.07 (dd, 14.5, 6.8)
11b	2.32 m	1.16 m	1.43 (dd, 14.5, 11.7)	1.43 (dd, 14.5, 11.7)
12a	2.56 (t, 13.6)	2.17 m	2.37 m	2.40 (dd, 14.2, 11.7)
12b	1.47 (dd, 14.7, 6.3)	1.34 (dd, 14.7, 6.5)	1.54 m	1.49 (dd, 14.2, 6.8)
16	1.51 (d, 8.8)	0.94 (d, 8.8)	1.52 m	1.54 (d, 9.3)
17	0.86 (dd, 11.2, 8.8)	0.68 (dd, 11.1, 8.8)	0.98 m	0.91 (dd, 10.8, 9.3)
18	0.96 s	0.96 s	1.06 s	1.03 (s)
19	4.39 (d, 7.6)	3.97 m	4.59 (d, 7.2)	4.58 (d, 7.2)
20	3.75 (dt, 11.3, 7.2)	2.99 m	3.07 m	3.16 m
21	1.79 (d, 6.5)	1.27 m	1.65 (d, 6.7)	1.71 (d, 6.7)
22	5.18 (dd, 8.3, 2.3)	4.75 (dd, 7.4, 2.8)	5.09 m	5.23 (dd, 9.0, 2.0)
23	5.43 q (2.1)	4.78 m	4.79 m	5.27 q (2.0)
24a	7.11 (d, 1.7)	2.19 m	2.16 m	7.09 (d, 1.7)
24b		2.08 m	1.88 m	
25		2.71 m	2.75 m	
27	1.84 (d, 1.8)	1.18 (d, 7.3)	1.17 (d, 7.3)	1.86 (d, 1.8)
29	1.38 s	1.29 s	1.31 s	1.32 s
30	1.21 s	1.27 s	1.22 s	1.23 s
-OAc	2.03 s	2.08 s	2.00 s	1.83 s
-OH	7.64 s (HO-8) 7.98 (d, 7.7) (HO-19) 9.08 s (HO-15)	7.36 s (HO-1)	8.52 (d, 7.2) (HO-19)	8.69 (d, 7.2) (HO-19)

[a] Recorded in pyridine-d_5; [b] Recorded in acetone-d_6

In consideration of the benefits of *Schisandra* species on human's nervous system, a few isolated SNTs were subjected to two PC12 cell related bioassays to evaluate their neurite outgrowth-promoting activities, and protective activities against neural injuries. As a result, preschisanartanins R (**2**), T (**4**), J (**13**), and A (**18**) were found to exhibit moderate cellular differentiation promoting effects in PC12 cells (Table 6 and Fig. S2). Moreover, preschisanartanin R (**2**) (10 μmol·L^{-1}) can prevent corticosterone-induced apoptosis in PC12 cells with survival ratio being 66% in 48 h (positive control: 10 μmol·L^{-1} desipramine; survival ratio: 81.7%) (Table S10).

Conclusion

Phytochemical investigation on two *Schisandra* species resulted in the isolation nineteen preschisanartane-type SNTs, which further manifested the structural diversity and complexity of SNTs, as well as their potential in combating neurodegenerative diseases. The originally proposed structure of

Table 5 ^{1}H NMR (600 MHz) data for compounds 9–11 (recorded in pyridine-d_5)

Position	**9**	**10**	**11**
1	5.19 s	5.16 (d, 5.6)	5.08 m
2a	4.61 (d, 3.5)	2.67 (d, 17.8)	3.36 m
2b		3.36 (dd, 17.8, 5.6)	2.75 (dd, 17.9, 1.5)
5	2.99 (dd, 12.6, 4.4)	2.91 m	2.40 (dd, 13.0, 3.9)
6a	2.38 m	2.33 m	2.94 m
6b	1.56 m	1.55 m	1.97 (dd, 13.0, 4.3)
7a	2.42 m	2.37 m	4.89 (t, 10.0)
7b	2.05 m	2.01 m	
8	2.93 (dd, 12.5, 5.4)	2.90 m	3.14 (dd, 10.1, 1.8)
11a	2.81 (dd, 15.3, 6.5)	2.82 m	2.78 m
11b	1.55 m	1.52 m	1.58 m
12a	2.29 m	2.53 (t, 13.4)	2.51 (t, 13.6)
12b	1.40 (dd, 14.4, 6.5)	1.43 overlap	1.39 m
16	1.50 m	1.43 overlap	1.57 m
17	1.04 m	0.92 (dd, 11.2, 8.9)	0.86 (t, 9.9)
18	1.02 s	0.98 s	0.97 s
19	4.64 (d, 7.7)	4.27 (d, 7.7)	4.28 (d, 6.7)
20	3.32 (dt, 12.2, 6.7)	3.60 m	3.71 m
21	1.80 (d, 6.7)	1.71 (d, 6.6)	1.75 (dd, 6.6)
22	5.22 (t, 5.6)	5.03 m	5.14 m
23	4.87 m	4.97 (dt, 8.5, 3.2)	5.40 s
24a	2.31 m	1.93 m	7.11 (t, 1.8)
24b	1.95 m	2.16 m	
25	2.74, m	2.80 m	
27	1.14 (d, 7.2)	1.19 (d, 7.3)	1.83 (d, 1.8)
29	1.48 s	1.48 s	1.36 s
30a	3.63 (d, 11.9)	3.64 (d, 11.8)	1.19 s
30b	3.81 (d, 11.9)	3.80 (d, 11.8)	
-OAc	2.10 s	2.14 s	2.01 s
-OH	8.64 (d, 7.8) (HO-19)	8.41 (d, 7.7) (HO-19)	8.46, m (HO-19)

Table 6 Neurite outgrowth-promoting activities of 4 SNTs [a]

Groups [b]	Samples	Concentrations	Differentiational ratio (72 h)
Group 1	Blank	/	No differentiation
	Negative control	5 ng·mL^{-1} NGF [c]	4.31%
	Positive control	50 ng·mL^{-1} NGF	21.94%
	2	10 μmol·L^{-1}	9.03%
Group 2	Blank	/	No differentiation
	Negative control	5 ng·mL^{-1} NGF	4.29%
	Positive control	50 ng·mL^{-1} NGF	18.82%
	4	10 μmol·L^{-1}	9.68%
	13	10 μmol·L^{-1}	11.54%
	18	10 μmol·L^{-1}	11.02%

[a] For bioactivity evaluation results of other SNTs, see Tables S8–S9; [b] Data were divided into groups because bioactivity evolution were undertaken in two separate batches; [c] NGF: nerve growth factor

preschisanartanin J was revised in the current research, however, it should be noted that structural misassignment is not a unique problem for SNTs. In fact, according to our own statistics, the proposed structures of over 100 natural products were revised during 2018. This situation not only calls for our rational use of the routinely available tools for structural determination, but also demands us to explore more advanced tools, such as the quantum chemical calculation method [23-24], anisotropic NMR spectroscopy [25-26], crystalline sponge method [27], etc.

Experimental

General experimental procedures

1D and 2D NMR spectra were recorded on Bruker AVANCE 600 and AVANCE 800 MHz NMR spectrometers. Chemical shifts (δ) were given on parts per million (ppm) scale with reference to the solvent signals and coupling constants were expressed in Hertz. ESI-MS and HRESI-MS were performed on Agilent Q-TOF mass spectrometer. UV data were recorded from 195 to 400 nm in MeOH using a Shimadzu UV-2401 PC spectrophotometer. Experimental ECD spectra were measured from 195 to 400 nm in MeOH using an Applied Photophysics spectrometer. IR spectra were recorded on a Tensor 27 spectrophotometer in KBr discs. Single-crystal X-ray data collected on a Bruker APEX DUO diffractometer using Cu Kα radiation at 100 K. Column chromatography was performed with silica gel (200−300 mesh), Lichroprep RP-18 gel (40−63 mm), MCI gel (75−150 mm), and Sephadex LH-20 gel (40−70 mm). Preparative HPLC (Agilent) with DAD detector was performed using an ODS column (7 μm, 21.2 mm × 25 cm, 20 mL·min^{-1}). Semi-preparative HPLC (Agilent) with a DAD detector was performed using an ODS column (5 μm, 9.4 mm × 25 cm, 3 mL·min^{-1}). Fractions were monitored by TLC, and spots were visualized by heating silica gel plates sprayed with 10% H_2SO_4 in EtOH. All solvents were distilled prior to use.

Plant material

The leaves and stems of *S. sphaerandra* were collected from the Maguan county, Wenshan prefecture of Yunnan Province, China, in August 2011. Voucher specimens (KIB 2011081601) were deposited at State Key Laboratory of Phytochemistry and Plant Resources in West China, Kunming Institute of Botany (KIB), Chinese Academy of Sciences (CAS), and were identified by Prof. LI Heng (Kunming Institute of Botany, Chinese Academy of Sciences).

The leaves and stems of *S. rubriflora* were collected from the Cangshan county, Dali prefecture of Yunnan Province, China, in September 2015. Voucher specimens (KIB2015091401) were deposited at State Key Laboratory of Phytochemistry and Plant Resources in West China, Kunming Institute of Botany (KIB), Chinese Academy of Sciences (CAS), and were identified by Prof. LI Heng (Kunming Institute of Botany, Chinese Academy of Sciences).

Extraction, isolation, and purification

The air-dried and powdered leaves and stems of *S. sphaerandra* (40 kg) and *S. rubriflora* (43 kg) were extracted with 70% aqueous Me_2CO (3 × 200 L, 3 days each) at room temperature, respectively. The extracting solutions were concentrated under reduced pressure to give crude extract, which was partitioned between H_2O and EtOAc. The EtOAc part (1580 g for *S. sphaerandra*; 1600 g for *S. rubriflora*) was chromatographed on a silica gel column with a gradient elution of $CHCl_3$/Me_2CO (1 : 0 to 0 : 1) to furnish six fractions, respectively (Fr SA–SF for *S. sphaerandra*, and Fr RA–RF for *S. rubriflora*).

Fration SD (90 g) was chromatographed with a gradient elution of MeOH/H_2O (3 : 7 to 1 : 0) on RP-18 to obtain fractions SD1–SD6. Fraction SD2 was chromatographed on Sephadex LH-20 eluting with MeOH/$CHCl_3$ (1 : 1) to afford 5 fractions (SD2a–SD2e). Fraction SD2c was chromatographed by a silica gel column (petroleum ether/Me_2CO_3 8 : 1 to 1 : 0) to give 8 fractions. Fraction SD2c2 was successively subjected to preparative TLC and semipreparative HPLC (3 mL·min^{-1}, detector UV λ_{max} 280 nm, MeCN/H_2O 2.8 : 7.2) and to yield **3** (2.0 mg), **4** (2.1 mg), **5** (1.0 mg). Fraction SD2c3 was successively subjected to preparative TLC and semipreparative HPLC (3 mL·min^{-1}, detector UV λ_{max} 280 nm, MeCN/H_2O 2.4 : 7.6) and to yield **11** (1.0 mg), **19** (4.8 mg). Fraction SD2c5 was subjected to semipreparative HPLC (3 mL·min^{-1}, detector UV λ_{max} 280 nm, MeCN/H_2O 3.0 : 7.0) and to yield **22** (3.4 mg), **16** (12.4 mg). Fraction SD2c8 was subjected to semipreparative HPLC (3 mL·min^{-1}, detector UV λ_{max} 280 nm, *n*-hexane/isopropanol/MeOH 78.5 : 18.5 : 3.5) and to yield **9** (2.5 mg), **10** (2.4 mg). Fraction SD3 was chromatographed by a silica gel column (petroleum ether/Me_2CO_3 8 : 1 to 1 : 0) to give 8 fractions (SD3a–3h). SD3a was successively subjected to Sephadex LH-20, preparative and semipreparative HPLC (3 mL·min^{-1}, detector UV λ_{max} 280 nm, MeCN/H_2O 4.0 : 6.0) to obtain **20** (3.5 mg), **21** (10 mg). SD3b was successively subjected to silica gel column and semipreparative HPLC (3 mL·min^{-1}, detector UV λ_{max} 280 nm, MeCN/H_2O 4.5 : 5.5) to obtain **7** (15.0 mg), **8** (5.0 mg). Fraction SD3 was chromatographed by a silica gel column (petroleum ether/Me_2CO_3 8 : 1 to 1 : 0) to give 5 fractions (SD3a–SD3e). Fraction SD3d was chromatographed on an ODS column to afford 6 fractions (SD3d1–SD3d6). Fraction SD3d3 was subjected to semipreparative HPLC (3 mL·min^{-1}, detector UV λ_{max} 280 nm, *n*-hexane/isopropanol/MeOH 82.5 : 15.0 : 2.5) and to yield **18** (5.0 mg), **15** (6.0 mg). Fraction SD3d3 was subjected to semipreparative HPLC (3 mL·min^{-1}, detector UV λ_{max} 280 nm, MeCN/H2O 4.0 : 6.0 to 6.0 : 4.0) to yield **2** (3.2 mg) and **6** (12.0 mg).

Fraction RD (62 g) was chromatographed with a gradient elution of MeOH/H_2O (3 : 7 to 1 : 0) on RP-18 to obtain fractions RD1–RD6. Fraction RD3 was chromatographed on Sephadex LH-20 eluting with MeOH/$CHCl_3$ (1 : 1) to afford 4 fractions (RD3a–RD3d). Fraction RD3c was successively subjected to preparative HPLC and semipreparative HPLC (3 mL·min^{-1}, detector UV λ_{max} 280 nm, MeOH/H_2O 4.5 : 5.5) to obtain **1** (3.3 mg). Fraction RD4 was chromatographed on Sephadex LH-20 eluting with MeOH/$CHCl_3$ (1 : 1) to afford 5 fractions (RD4a–RD4e). Fraction RD4d was subjected to

semipreparative HPLC (3 mL·min^{-1}, detector UV λ_{max} 280 nm, MeCN/H2O 4.0 : 6.0) to obtain **12** (5.0 mg).

Preschisanartanin Q (**1**): White powder; $[\alpha]_D^{19.4}$ −56.1 (*c* 0.034, MeOH); UV (MeOH) λ_{max} (log ε) 210.8 (4.02) nm; ECD (MeOH) λ_{max} ($\Delta\varepsilon$) 213 (−1.02) nm; IR (KBr) ν_{max} 3433.06, 2970.75, 2929.09, 2874.47, 1758.54, 1633.79 cm^{-1}; For ^{1}H and ^{13}C NMR data, see Tables 2 and 3; HRESI-MS *m/z* 553.2408 $[M + Na]^+$ (Calcd. for $C_{29}H_{38}O_9Na$, 553.2408).

Preschisanartanin R (**2**): White powder; $[\alpha]_D^{24.0}$ −48.3 (*c* 0.121, MeOH); UV (MeOH) λ_{max} (log ε) 210.0 (4.13) nm; ECD (MeOH) λ_{max} ($\Delta\varepsilon$) 214 (−2.05) nm; IR (KBr) ν_{max} 3431.48, 2969.92, 2932.52, 2872.11, 1755.33, 1631.45 cm^{-1}; For ^{1}H and ^{13}C NMR data, see Tables 2 and 3; HRESI-MS (*m/z* 613.2413 $[M + K]^+$, Calcd. for $C_{31}H_{42}O_{10}K$, 613.2410).

Preschisanartanin S (**3**): White powder; $[\alpha]_D^{19.3}$ +5.8 (*c* 0.11, MeOH); UV (MeOH) λ_{max} (log ε) 203.0 (3.54) nm, 248.0 (2.74) nm; For ^{1}H and ^{13}C NMR data, see Tables 2 and 3; HRESI-MS (*m/z* 645.2511 $[M + Na]^+$, Calcd. for $C_{31}H_{42}O_{13}Na$, 645.2518).

Preschisanartanin T (**4**): White powder; $[\alpha]_D^{23.5}$ +3.2 (*c* 0.123, MeOH); UV (MeOH) λ_{max} (log ε) 205.5 (3.63) nm; IR (KBr) ν_{max} 3434.34, 2969.84, 2934.17, 2878.20, 1772.59, 1740.40, 1631.44 cm^{-1}; For ^{1}H and ^{13}C NMR data, see Tables 2 and 3; HRESI-MS (*m/z* 605.2610 $[M + Na]^+$, Calcd. for $C_{31}H_{42}O_{12}Na$, 605.2604).

Preschisanartanin U (**5**): White powder; $[\alpha]_D^{24.1}$ −16.7 (*c* 0.118, MeOH); UV (MeOH) λ_{max} (log ε) 208.5 (3.99) nm, 277.5 (2.53) nm; ECD (MeOH) λ_{max} ($\Delta\varepsilon$) 210 (−1.15) nm, 328 (−2.08) nm; IR (KBr) ν_{max} 3432.15, 2969.28, 2930.61, 2873.33, 1769.21, 1628.53 cm^{-1}; For ^{1}H and ^{13}C NMR data, see Tables 2 and 4; HRESI-MS (*m/z* 717.2384 $[M + CF_3COO]^-$, Calcd. for $C_{33}H_{40}O_{14}F_3$, 717.2376).

Preschisanartanin V (**6**): White powder; $[\alpha]_D^{23.6}$ −2.1 (*c* 0.09, MeOH); UV (MeOH) λ_{max} (log ε) 204.0 (3.69) nm; IR (KBr) ν_{max} 3436.91, 2970.71, 2933.53, 2872.75, 1765.83; 1630.09 cm^{-1}; For ^{1}H and ^{13}C NMR data, see Tables 2 and 4; HRESI-MS (*m/z* 605.2617 $[M - H]^-$, Calcd. for $C_{31}H_{41}O_{12}$, 605.2604).

Preschisanartanin W (**7**): White powder; $[\alpha]_D^{23.5}$ +45.8 (*c* 0.204, MeOH); UV (MeOH) λ_{max} (log ε) 205.0 (3.62) nm; IR (KBr) ν_{max} 3431.47, 2973.02, 2936.58, 2877.57, 1772.07, 1631.48 cm^{-1}; For ^{1}H and ^{13}C NMR data, see Tables 2 and 4; HRESI-MS (*m/z* 625.2433 $[M + Cl]^-$, Calcd. for $C_{31}H_{42}O_{11}Cl$, 625.2411).

Preschisanartanin X (**8**): White powder; $[\alpha]_D^{23.8}$ +12.6 (*c* 0.113, MeOH); UV (MeOH) λ_{max} (log ε) 204.5 (4.01) nm, 270.5 (3.12) nm; ECD (MeOH) λ_{max} ($\Delta\varepsilon$) 215 (−0.44) nm; IR (KBr) ν_{max} 3431.82, 2968.53, 2931.79, 2875.71, 1759.88, 1744.02, 1630.35 cm^{-1}; For ^{1}H and ^{13}C NMR data, see Tables 2 and 4; HRESI-MS (*m/z* 623.2259 $[M + Cl]^-$, Calcd. for $C_{31}H_{40}O_{11}Cl$, 623.2265).

Preschisanartanin Y (**9**): White powder; $[\alpha]_D^{23.7}$ +4.9 (*c* 0.198, MeOH); UV (MeOH) λ_{max} (log ε) 207.5 (3.31) nm, 277.0 (2.70) nm; IR (KBr) ν_{max} 3425.15, 2961.53, 2935.68, 2873.06, 1763.63, 1631.47 cm^{-1}; For ^{1}H and ^{13}C NMR data, see Tables 2 and 5; HRESI-MS (*m/z* 645.2517 $[M + Na]^+$, calcd for $C_{31}H_{42}O_{13}Na$, 645.2518).

Preschisanartanin Z (**10**): White powder; $[\alpha]_D^{23.6}$ +20.6 (*c* 0.14, MeOH); UV (MeOH) λ_{max} (log ε) 204.8 (3.58) nm, 273.0 (2.56) nm; IR (KBr) ν_{max} 3439.83, 2932.81, 2872.00, 1763.25, 1632.10 cm^{-1}; For ^{1}H and ^{13}C NMR data, see Tables 2 and 5; HRESI-MS (*m/z* 629.2564 $[M + Na]^+$, Calcd. for $C_{31}H_{42}O_{12}Na$, 629.2568).

Preschidilactone A (**11**): White powder; $[\alpha]_D^{22.7}$ +18.8 (*c* 0.154, MeOH); UV (MeOH) λ_{max} (log ε) 208.0 (4.00) nm, 276.0 (3.25) nm; ECD (MeOH) λ_{max} ($\Delta\varepsilon$) 214 (−1.04) nm, 323 (−0.33) nm; IR (KBr) ν_{max} 3438.17, 2969.21, 2931.01, 2872.74, 1758.97, 1632.05 cm^{-1}; For ^{1}H and ^{13}C NMR data, see Tables 2 and 5; HRESI-MS (*m/z* 627.2421 $[M + Na]^+$, Calcd. for $C_{31}H_{40}O_{12}Na$, 627.2412).

Computational method

Conformational analysis of molecules was initially performed in Spartan'16 (Wavenfunction, Irvine, 2016, CA, USA) using the Monte Carlo algorithm and Merck molecular force field (MMFF). Those obtained conformers within 5 kcal·mol^{-1} were subjected to DFT geometry optimization at B3LYP/6-31G(d) level of theory. Frequency analysis of all optimized conformations were undertaken at the same level of theory to ensure they were true local minima on the potential energy surface, as well as to obtain the Gibbs free energy of each conformer. Room-temperature (298.15 K) equilibrium populations were calculated according to Boltzmann distribution law:

$$p_i = \frac{n_i}{\sum_j n_j} = \frac{e^{-\Delta G_i/RT}}{\sum_j e^{-\Delta G_j/RT}} \frac{Q_{i(\text{Relative})}}{Q_{(\text{Relative})}}$$

Where P_i is the population of the i^{th} conformer; n_i the number of molecules in i^{th} conformer; ΔG is the relative Gibbs free energy (kcal·mol^{-1}); T is the temperature, usually the room temperature (298.15 K); R is the ideal gas constant (0.001 985 899 5); Q is the partition function. Those conformers with population over 1% were subjected to subsequent calculations.

NMR shielding constants were calculated with the GIAO method at mPW1PW91-SCRF/6-31G(d, p) level with IEFPCM solvent model in corresponding solvent. The shielding constants obtained were converted into chemical shifts by referencing to TMS at 0 ppm ($\delta_{cal} = \sigma_{TMS} - \sigma_{cal}$), where the σ_{TMS} was the shielding constant of TMS calculated at the same level. For each possible candidate, the parameters a and b of the linear regression $\delta_{cal} = a\delta_{exp} + b$; the correlation coefficient, R^2; the mean absolute error (MAE) defined as $\Sigma_n |\delta_{cal} - \delta_{exp}|/n$; the corrected mean absolute error, CMAE, defined as $\Sigma_n |\delta_{corr} - \delta_{exp}|/n$, where $\delta_{corr} = (\delta_{cal} - b)/a$, were calculated [28]. The DP4+ probabilities of each possible candidate were calculated with the EXCEL spreadsheet provided by Sarotti, *et al*. [22]. Spin-spin coupling constants (SSCC) were calculated using method recommended by Bally & Rablen [29]. The geometry optimization, frequency analysis, calculation of NMR shielding constants, and SSCC calculation were all carried out using

the Gaussian 09 software package (Revision E.01. Gaussian, Inc., Wallingford CT, 2013).

Supporting Information

Supporting information of this paper can be downloaded at the following link (https://pan.baidu.com/s/1vADmCX8zIQHIrbEb90IS0g) or be requested by sending E-mails to the corresponding author.

References

[1] Xiao WL, Li RT, Huang SX, *et al*. Triterpenoids from the Schisandraceae family [J]. *Nat Prod Rep*, 2008, **25**(5): 871-891.

[2] Shi YM, Xiao WL, Pu JX, *et al*. Triterpenoids from the Schisandraceae family: an update [J]. *Nat Prod Rep*, 2015, **32**(3): 367-410.

[3] Li RT, Zhao QS, Li SH, *et al*. Micrandilactone A: a novel triterpene from *Schisandra micrantha* [J]. *Org Lett*, 2003, **5**(7): 1023-1026.

[4] Li RT, Zhao QS, Li SH, *et al*. Micrandilactone A: a novel triterpene from *Schisandra micrantha*. [Erratum to document cited in CA138: 365526] [J]. *Org Lett*, 2006, **8**(4): 801.

[5] Li X, Cheong PH, Carter RG. Schinortriterpenoids: a case study in synthetic design [J]. *Angew Chem Int Ed*, 2017, **56**(7): 1704-1718.

[6] Yang Z. The journey of schinortriterpenoid total syntheses [J]. *Acc Chem Res*, 2019, **52**(2): 480-491.

[7] Xiao WL, Yang LM, Gong NB, *et al*. Rubriflordilactones A and B, two novel bisnortriterpenoids from *Schisandra rubriflora* and their biological activities [J]. *Org Lett*, 2006, **8**(5): 991-994.

[8] Yang P, Yao M, Li J, *et al*. Total synthesis of rubriflordilactone B [J]. *Angew Chem Int Ed*, 2016, **55**(24): 6964-6968.

[9] Lei C, Huang SX, Chen JJ, *et al*. Propindilactones E–J, schiartane nortriterpenoids from *Schisandra propinqua* var. *propinqua* [J]. *J Nat Prod*, 2008, **71**(7): 1228-1232.

[10] You L, Liang XT, Xu LM, *et al*. Asymmetric total synthesis of propindilactone G [J]. *J Am Chem Soc*, 2015, **137**(32): 10120-10123.

[11] Shi YM, Hu K, Pescitelli G, *et al*. Schinortriterpenoids with identical configuration but distinct ECD spectra generated by nondegenerate exciton coupling [J]. *Org Lett*, 2018, **20**(6): 1500-1504.

[12] Cheng YB, Liao TC, Luo YW, *et al*. Nortriterpene lactones from the fruits of *Schisandra arisanensis* [J]. *J Nat Prod*, 2010, **73**(7): 1228-1233.

[13] Liu Y, Tian T, Yu HY, *et al*. Nortriterpenoids from the stems and leaves of *Schisandra viridis* [J]. *Fitoterapia*, 2017, **118**: 38-41.

[14] He F, Li XY, Yang GY, *et al*. Nortriterpene constituents from *Schisandra sphenanthera* [J]. *Tetrahedron*, 2012, **68**(2): 440-446.

[15] Huang SX, Han QB, Lei C, *et al*. Isolation and characterization of miscellaneous terpenoids of *Schisandra chinensis* [J]. *Tetrahedron*, 2008, **64**(19): 4260-4267.

[16] Gao XM, Li YQ, Shu LD, *et al*. New triterpenoids from the fruits of *Schisandra wilsoniana* and their biological activities [J]. *Bull Korean Chem Soc*, 2013, **34**(3): 827-830.

[17] Huang SX, Li RT, Liu JP, *et al*. Isolation and characterization of biogenetically related highly oxygenated nortriterpenoids from *Schisandra chinensis* [J]. *Org Lett*, 2007, **9**(11): 2079-2082.

[18] Lei C, Xiao WL, Huang SX, *et al*. Pre-schisanartanins C−D and propintrilactones A−B, two classes of new nortriterpenoids from *Schisandra propinqua* var. *propinqua* [J]. *Tetrahedron*, 2010, **66**(13): 2306-2310.

[19] Shi YM, Wang XB, Li XN, *et al*. Lancolides, antiplatelet aggregation nortriterpenoids with tricyclo[6.3.0.02, 11]undecane-bridged system from *Schisandra lancifolia* [J]. *Org Lett*, 2013, **15**(19): 5068-5071.

[20] Jayanetti DR, Yue Q, Bills GF, *et al*. Hypocoprins A–C: new sesquiterpenoids from the *Coprophilous fungus* hypocopra rostrata [J]. *J Nat Prod*, 2015, **78**(3): 396-401.

[21] Shi YM, Wang LY, Zou XS, *et al*. Nortriterpenoids from *Schisandra chinensis* and their absolute configurational assignments by electronic circular dichroism study [J]. *Tetrahedron*, 2014, **70**(4): 859-868.

[22] Grimblat N, Zanardi MM, Sarotti AM. Beyond DP4: an improved probability for the stereochemical assignment of isomeric compounds using quantum chemical calculations of NMR shifts [J]. *J Org Chem*, 2015, **80**(24): 12526-12534.

[23] Lodewyk MW, Siebert MR, Tantillo DJ. Computational prediction of ^{1}H and ^{13}C chemical shifts: A useful tool for natural product, mechanistic, and synthetic organic chemistry [J]. *Chem Rev*, 2012, **112**(3): 1839-1862.

[24] Grauso L, Teta R, Esposito G, *et al*. Computational prediction of chiroptical properties in structure elucidation of natural products [J]. *Nat Prod Rep*, 2019, **36**(7): 1005-1030.

[25] Liu Y, Saurí J, Mevers E, *et al*. Unequivocal determination of complex molecular structures using anisotropic NMR measurements [J]. *Science*, 2017, **356**(6333): eaam5349.

[26] Li GW, Liu H, Qiu F, *et al*. Residual dipolar couplings in structure determination of natural products [J]. *Nat Prod Bioprospect*, 2018, **8**(4): 279-295.

[27] Inokuma Y, Yoshioka S, Ariyoshi J, *et al*. X-ray analysis on the nanogram to microgram scale using porous complexes [J]. *Nature*, 2013, **495**: 461-466.

[28] Willoughby P, Jansma M, Hoye T. A guide to small-molecule structure assignment through computation of (^{1}H and ^{13}C) NMR chemical shifts [J]. *Nat Protoc*, 2014, **9**(3): 643-660.

[29] Bally T, Rablen PR. Quantum-chemical simulation of ^{1}H NMR spectra. 2. Comparison of DFT-based procedures for computing proton-proton coupling constants in organic molecules [J]. *J Org Chem*, 2011, **76**(12): 4818-4830.

Cite this article as: HU Kun, LI Xing-Ren, TANG Jian-Wei, Li Xiao-Nian, PUNO Pema-Tenzin. Structural determination of eleven new preschisanartane-type schinortriterpenoids from two *Schisandra* species and structural revision of preschisanartanin J using NMR computation method [J]. *Chin J Nat Med*, 2019, **17**(12): 970-981.

Prof. Puno Pema-Tenzin, Kunming Institute of Botany, Chinese Academy of Sciences

Prof. Puno Pema-Tenzin is mainly engaged in the research of Natural Products Chemistry, and majorly focused on the basic and applied basic research for the secondary metabolites and their bioactivities from two economically and medicinally important phytogroup (Schisandraceae and *Isodon*) and their endophytic fungi.